Journal of Geochemical Exploration 106 (2010) 219–225

Contents lists available at ScienceDirect

Journal of Geochemical Exploration

journal homepage: www.elsevier.com/locate/jgeoexp

Modeling chemical and phase equilibria in geochemical systems using a speciation-based model

Peiming Wang *, Andrzej Anderko, Ronald D. Springer, Jerzy J. Kosinski, Malgorzata M. Lencka

OLI Systems, Inc., 108 American Road, Morris Plains, NJ 07950, USA

ARTICLE INFO

Article history:
Received 6 April 2009
Accepted 3 September 2009
Available online 21 September 2009

Keywords:
Phase equilibria
Solubility
Speciation
Thermodynamic model
Transition metal

ABSTRACT

A comprehensive thermodynamic model has been applied to calculating phase equilibria, speciation, and other thermodynamic properties of systems that are of geochemical importance. The analyzed systems are relevant to the mineralization of Pb, Ni, Cu, Zn, and Fe. The thermodynamic framework is based on a previously developed model for mixed-solvent electrolyte solutions. The framework has been designed to reproduce the properties of salt solutions at temperatures ranging from the freezing point to 300 °C and for concentrations ranging from infinite dilution to the fused salt limit. The accuracy of the model has been demonstrated by calculating solubilities in multicomponent solutions and predicting the effects of chemical speciation, pH, temperature, CO_2 partial pressure, and concentrations of acids, bases, and selected salts on the formation of various solid phases.

1. Introduction

Electrolyte thermodynamics is of great importance for understanding and being able to simulate various processes that involve mineralizing environments and hydrometallurgical systems. In such systems, multicomponent electrolyte solutions are encountered at high concentrations under diverse conditions of temperature and pressure. Solutions of this nature are challenging for computational models because of their complex chemical behavior and strong nonideality. A self-consistent treatment of speciation and phase equilibria is of utmost importance for realistic simulation of electrolyte systems because phase equilibria and other thermodynamic properties are often inextricably linked to speciation equilibria due to ion pairing, hydrolysis, acid–base reactions, and other phenomena.

Recently, a general, speciation-based thermodynamic model for mixed-solvent electrolyte solutions has been developed (Anderko, et al. 2002, Wang et al. 2002). This model was shown to reproduce simultaneously vapor–liquid, solid–liquid and liquid–liquid equilibria, speciation, caloric and volumetric properties of electrolytes in water, organic, or mixed solvents (Wang et al. 2004, 2006). The model is valid for salts from infinite dilution to the fused salt limit and for various completely miscible inorganic systems (such as acid–water mixtures) over a full concentration range (Kosinski et al. 2007). This is an important advantage over other available activity coefficient models, such as the well-known molality-based model of Pitzer (1991) which represents solution properties for concentrations up to only 6 m for most electrolyte solutions. Also, the model is capable of representing phase equilibria in multicomponent inorganic systems containing multiple salts, acids, and bases (Wang et al., 2004, 2005, Gruszkiewicz et al., 2007). Applications of this model to hydrometallurgical systems have been reported previously (Liu and Papangelakis, 2005, 2006; Azimi et al, 2007, 2008). Complex phase behavior such as the formation of multiple hydrated salts, double salts, or the presence of eutectic points has been accurately represented. The model is referred to as the mixed-solvent electrolyte (MSE) model because it is equally valid for classical aqueous systems, those with more than one distinct solvent and mixtures in which a given component may continuously vary from being a solute to being a solvent (e.g., in acid–water mixtures).

In this study, we examine the applicability of this model to selected systems that are of geochemical and hydrometallurgical interest. In particular, solutions involving transition and post-transition metals are analyzed because they constitute an important class of systems for these applications. Rather than focusing on particular processes, the current work is to provide a stringent test for the model on the basis of the available experimental thermodynamic data for such systems. The model is used to represent the properties of multicomponent aqueous solutions containing metal oxides, sulphides, sulphates, chlorides, carbonates, and nitrates in the presence of other salts and acids. It is applied to reproduce the effect of system variables such as temperature, pH, salt or acid concentration, and CO_2 partial pressure on the solubility behavior of various solids. In particular, solubilities of solids in mixed water–acid solutions are examined in the full range of acid concentration. These results can provide a thermodynamic foundation to explain natural variations in mineral deposits and to evaluate how the physicochemical properties of mineralizing solutions may affect the hydrothermal deposit formation.

* Corresponding author. Tel.: +1 973 539 4996; fax: +1 973 539 5922.
E-mail address: pwang@olisystems.com (P. Wang).

0375-6742/$ – see front matter
doi:10.1016/j.gexplo.2009.09.003

2. Thermodynamic model

Details of the thermodynamic model used in this study have been described elsewhere (Wang et al. 2002, 2004, 2006) and, therefore, only a brief summary is given here. The thermodynamic framework combines an excess Gibbs energy model for mixed-solvent electrolyte systems with a comprehensive treatment of chemical equilibria. The excess Gibbs energy is expressed as

$$\frac{G^{ex}}{RT} = \frac{G^{ex}_{LR}}{RT} + \frac{G^{ex}_{II}}{RT} + \frac{G^{ex}_{SR}}{RT} \quad (1)$$

where G^{ex}_{LR} represents the contribution of long-range electrostatic interactions, G^{ex}_{II} accounts for specific ionic (ion–ion and ion–molecule) interactions and G^{ex}_{SR} is a short-range contribution resulting from intermolecular interactions. The long-range interaction contribution is calculated from the Pitzer–Debye–Hückel formula (Pitzer, 1991) expressed in terms of mole fractions and symmetrically normalized. The short-range interaction contribution is calculated from the UNIQUAC equation (Abrams and Prausnitz, 1975). The specific ion-interaction contribution is calculated from an ionic strength-dependent, symmetrical second virial coefficient-type expression (Wang et al., 2002):

$$\frac{G^{ex}_{MR}}{RT} = -(\sum_i n_i)\sum_i \sum_j x_i x_j B_{ij}(I_x) \quad (2)$$

where $B_{ij}(I_x) = B_{ji}(I_x)$, $B_{ii} = B_{jj} = 0$ and the ionic strength dependence of B_{ij} is given by

$$B_{ij}(I_x) = b_{ij} + c_{ij}\exp(-\sqrt{I_x + a_1}) \quad (3)$$

where b_{ij} and c_{ij} are adjustable parameters and a_1 is set equal to 0.01. In general, the parameters b_{ij} and c_{ij} are calculated as functions of temperature as

$$b_{ij} = b_{0,ij} + b_{1,ij}T + b_{2,ij}/T \quad (4)$$

$$c_{ij} = c_{0,ij} + c_{1,ij}T + c_{2,ij}/T. \quad (5)$$

For electrolyte systems encountered in geochemical processes, the specific ion-interaction contribution is by far the most important one to reproduce the properties of the solutions. When a chemical process occurs in mixed solvents with organic components, the short-range contribution must also be introduced to account for the molecular interactions between solvent components.

While the excess Gibbs energy model is used to calculate nonideality effects on solution properties, the chemical equilibrium is governed by the chemical potentials of all species that participate in various reactions, such as precipitation, ion pairing or complexation. The chemical potential of each ionic or neutral species i is determined by its standard-state contribution, $\mu_i^0(T,P)$ and its activity coefficient, $\gamma_i(T,P,x)$, i.e.,

$$\mu_i(T,P,x) = \mu_i^0(T,P) + RT\ln x_i\gamma_i(T,P,x). \quad (6)$$

The standard-state chemical potentials of aqueous species, $\mu_i^0(T,P)$, are calculated as functions of temperature and pressure using the Helgeson–Kirkham–Flowers–Tanger (HKF) equation of state (Helgeson and Kirkham, 1974, 1976; Helgeson et al., 1981). The parameters of the HKF model are available for a large number of aqueous species including ions and ion pairs (e.g. Shock and Helgeson, 1988, Sverjensky et al. 1997). It should be noted that standard-state properties calculated from the model of Helgeson et al. are based on the infinite-dilution reference state and on the molality concentration scale. To make the equilibrium calculations consistent when the standard-state properties are combined with the mole fraction-based and symmetrically normalized activity coefficients, two conversions are performed: (1) the activity coefficients calculated from Eq. (1) are converted to those based on the unsymmetrical reference state, i.e., at infinite dilution in water and (2) the molality-based standard-state chemical potentials are converted to corresponding mole fraction-based quantities (Wang et al. 2002). For systems, in which the solution concentration approaches the infinite dilution limit, the standard-state properties, as calculated from the HKF equation of state, may be used alone to represent the solubility behavior or other solution properties. This can be exemplified by representing extremely low solubilities of minerals in water (*ca.* less than 10^{-5} m) without the presence of any other electrolyte component. The increased solubilities at higher solution concentrations such as those encountered in mineralizing and hydrometallurgical processes can only be accurately represented by combining the standard-state thermochemical properties with an appropriate activity coefficient model, as described above. Thus, the calculations are based on the combined usage of the originally reported HKF parameters for standard-state properties and the activity coefficient parameters as determined here.

3. Evaluation of model parameters

The parameters of the model are determined using thermodynamic data of various types, including: (1) vapor–liquid equilibria; (2) activity and osmotic coefficients; (3) solubility of salts in water or other solvents; (4) speciation data, such as pH and dissociation constants; (5) enthalpies of dilution or mixing; (6) heat capacities; and (7) densities.

The vapor–liquid equilibrium, activity and osmotic coefficient data constrain directly the excess Gibbs energy, whereas the solid–liquid equilibrium data can be used to constrain both the excess Gibbs energy and the properties of the solid phases that are in equilibrium with the liquid phase. The use of multiple data types is important to ensure the accuracy of model parameters. For example, caloric data (heat of mixing or dilution and heat capacities) are useful to determine the temperature dependence of model parameters. This makes it possible to make reliable predictions of solubilities well beyond the temperature range of experimental solubility data.

4. Results and discussion

Validation of the model for a number of fundamental electrolyte systems and multicomponent solutions has been reported previously (Wang et al., 2004, 2005, 2006; Kosinski et al., 2007). In this study, we examine systems containing selected transition and post-transition metals that are of importance in mineralization and hydrometallurgical processes. An important feature of transition metals is their strong tendency for hydrolysis and complex formation.

First, we apply the model to aqueous solutions containing metal oxides. Figs. 1 and 2 show the solubility results for CuO and NiO, respectively, as a function of pH and temperature. In both systems, the solubility markedly decreases with pH in acidic solutions and then increases after a minimum is reached. This solubility trend is strongly correlated to the hydrolysis of the metal cations (Baes and Mesmer, 1976). The effect of temperature on the solubility appears to be more pronounced for CuO compared with NiO. The solubility minimum for CuO is shifted to higher values as temperature rises, with an increase by more than two orders of magnitude from 25 °C to 300 °C. In contrast, the solubility minimum for NiO decreases, but only by one order of magnitude in the same temperature range. It should be noted that only the stable solid phases are presented in Figs. 1 and 2. For example, at 25 °C, the stable solid phase in nickel solutions is $Ni(OH)_2$, while NiO is the stable solid phase at higher temperatures (e.g. 150 °C and 300 °C). These solid phases are, therefore, shown in Fig. 2. CuO is more stable compared to $Cu(OH)_2$ at all the temperatures shown in Fig. 1. The model results are in good agreement with literature data

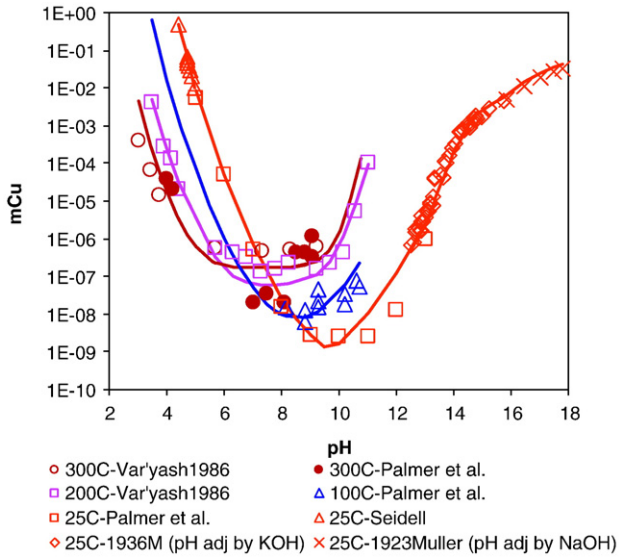

Fig. 1. Calculated and experimental solubilities of CuO as a function of pH at various temperatures. Experimental data are from Var'yash (1986), Petrov and Palmer (2000), Linke and Seidell (1965), McDowell and Johnston (1936), and Muller (1923). The lines are calculated from the model.

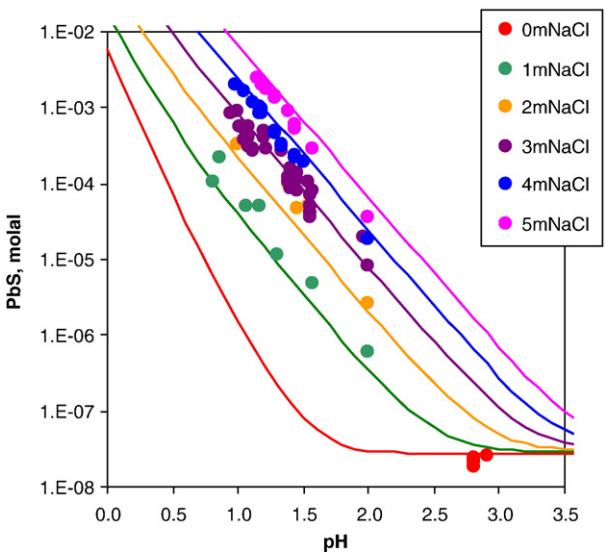

Fig. 3. Calculated and experimental solubilities of PbS (galena) in aqueous NaCl solutions saturated with H_2S at 1 atm at 80 °C and various NaCl concentrations. Experimental data are from Rafalskiy and Masalovich (1981), Barrett and Anderson (1982, 1988), and Anderson (1962).

within the experimental uncertainty. It should be noted that the pH values shown in Figs. 1 and 2 are those in the equilibrium solutions at the indicated temperatures. These pH values were either fixed by adjusting the amount of added base or acid, or were calculated at the given concentrations of the added base or acid. For example, the calculated pH is 17.8 in the saturated aqueous CuO solution when 25 m of NaOH is added at 25 °C.

Salt effects on the solubility of solids are of importance for understanding geochemical processes such as those related to hydrothermal brines, seawater systems, and evaporite formation. Therefore, the model has been applied to examine the effect of common salts on the solubilities of selected solids. Fig. 3 shows the solubility of lead sulfide (galena) in aqueous sodium chloride solutions saturated with H_2S at 1 atm at 80 °C. The solubility of PbS increases with added salt concentration. Addition of salt may also lead to more complex solubility behavior. Fig. 4 shows the effect of Na_2SO_4 on the solubility of $PbSO_4$ (anglesite). The solubility decreases drastically with added Na_2SO_4 at very low salt concentrations (e.g. $Na_2SO_4 < 0.001$ m), then it levels off as the salt concentration reaches ~0.01 m, and increases again with further additions of Na_2SO_4. The initial decrease in the solubility is due to the common-ion effect of SO_4^{-2}, which suppresses the dissolution of $PbSO_4$. As more Na_2SO_4 is

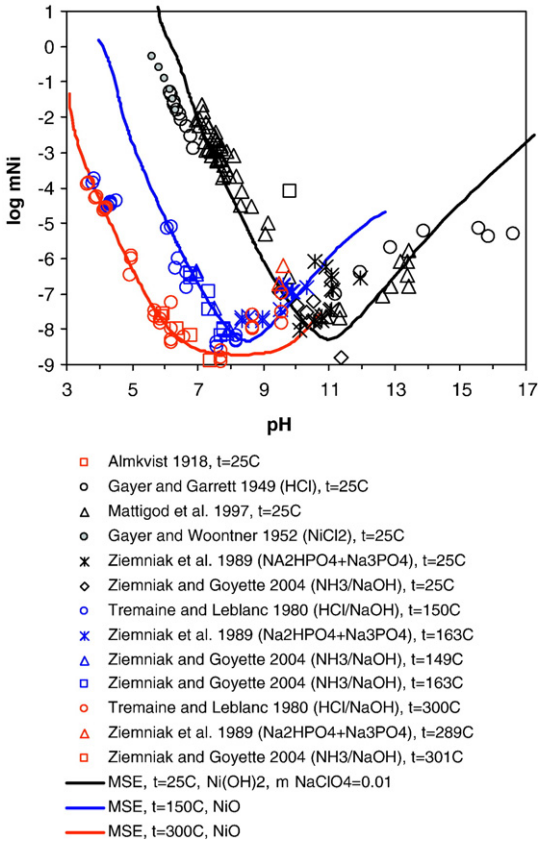

Fig. 2. Calculated and experimental solubilities of $NiO/Ni(OH)_2$ as a function of pH at various temperatures. Experimental data are from Almkvist (1918), Gayer and Garrett (1949), Mattigod et al. (1997), Gayer and Woontner (1952), Tremaine and Leblanc (1980), Ziemniak et al. (1989), Ziemniak and Goyette (2004). The lines are calculated from the model.

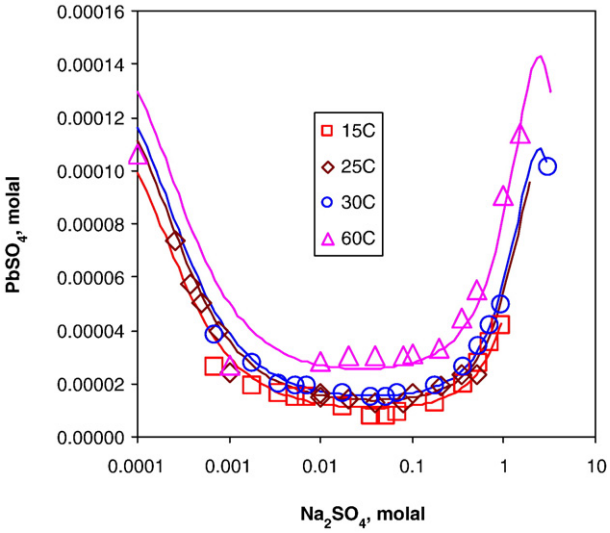

Fig. 4. Calculated and experimental solubility of $PbSO_4$ (anglesite) in aqueous Na_2SO_4 solutions. Experimental data are from Linke and Seidell (1965), Qiu et al. (2006), and Paige et al. (1992).

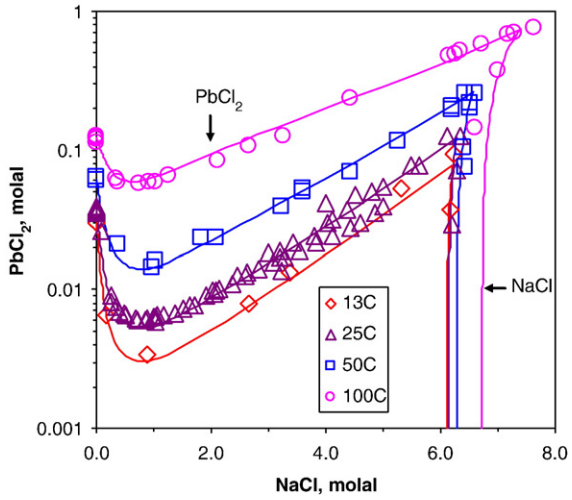

Fig. 5. Calculated and experimental solubilities in the $PbCl_2 + NaCl + H_2O$ system at various temperatures. Experimental data were taken from Linke and Seidell (1965), Tan et al. (1987), and Mgaidi et al. (1991).

added, a complex $PbSO_4^0$ is formed so that the Pb is dissolved into the solution in the form of complexes. A similar solubility behavior is seen in the system $PbCl_2 + NaCl + H_2O$ (Fig. 5). As NaCl concentration increases, there is a rapid decrease in the solubility of $PbCl_2$ in the relatively dilute region (i.e., for NaCl less than ~0.5 m). Then, after a minimum is reached in the intermediate NaCl concentrations (~1 m), the solubility increases due to the formation of complexes, $PbCl_n^{2-n}$ ($n = 1$–4). It is noteworthy that the $PbCl_2$ solubility curve is terminated by the precipitation of NaCl(s), which appears in equilibrium with the solution at very high NaCl concentrations (i.e. >6 m). The accurate representation of these solubility trends indicates that the model is capable of correctly predicting the nonideality of these systems.

After examining solubilities in aqueous salt systems, calculations have been performed for systems with mixed solvents consisting of an acid and water. In particular, we focused on strong acids such as H_2SO_4, HNO_3, and HCl, which are often used as leaching or oxidizing reagents in metal extraction processes. The model is applied to the entire solvent composition range, i.e. from pure water to the pure acid. Fig. 6 shows illustrative results for $PbSO_4$ solubility in $H_2SO_4 + H_2O$ mixtures. Complex phase behavior can be seen as the acid concentration goes from infinite dilution to pure H_2SO_4 (at which point the salt-free mole fraction of SO_3 is 0.5) and beyond, i.e. into the oleum ($SO_3 + H_2SO_4$) region. The results for $FeCl_3$ and $PbCl_2$ in aqueous HCl are shown in Figures 7a and b, respectively, and those for $Zn(NO_3)_2$ in aqueous HNO_3 are illustrated in Fig. 8. The solid phase in equilibrium with the solutions depends largely on the temperature and the acid concentration. At lower acid concentrations, hydrates with more hydrated water are formed. The number of hydration water molecules decreases with acid concentration, as shown in Figs. 7a and 8. Also, acid solvates, such as $FeCl_3 \cdot HCl$, can be formed at sufficiently high concentrations (i.e. for HCl concentration above 18 m). At elevated temperatures, only the hydrates with a reduced number of hydration water molecules precipitate, as demonstrated in Fig. 7a. The solubility in these systems shows a very complex behavior with multiple hydrates, anhydrous solids, and acid solvates formed as temperature and acid concentration change. These solubility patterns are determined by highly specific interactions between ions and solvent molecules, and have been accurately reproduced by the model.

The effect of partial pressure of CO_2 on the solubility of solids is of particular interest. Fig. 9 shows solubility of $PbCO_3$ (cerussite) as a function of P_{CO_2}. Results for $CaCO_3$ (calcite) and $MgCO_3$ (magnesite) are also included in this Fig. for comparison. An increase in partial pressure of CO_2 enhances the solubilities of these metal carbonates. In the presence of other salts, however, the dependence of the solubility

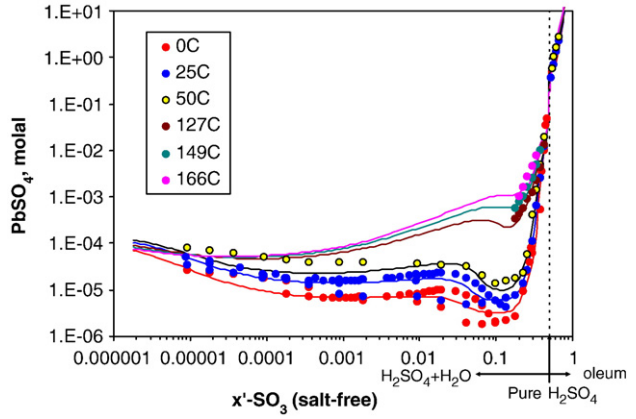

Fig. 6. Calculated and experimental solubility results for $PbSO_4$ (anglesite) in mixed sulfuric acid + water solvents at various temperatures. Experimental data are from Linke and Seidell (1965).

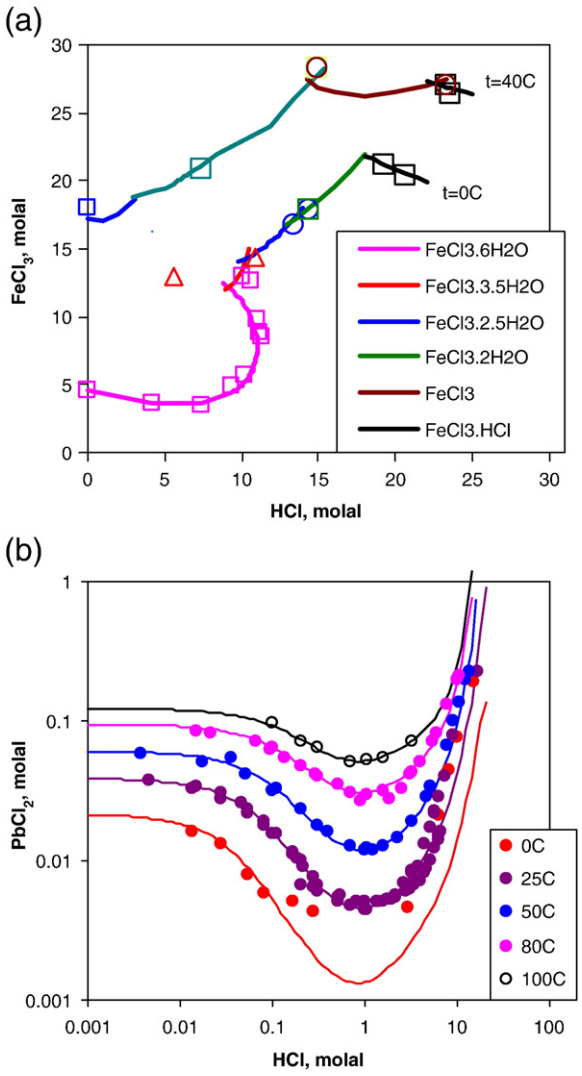

Fig. 7. Calculated and experimental solubilities in (a) the $FeCl_3 + HCl + H_2O$ system at 0 °C and 40 °C; and (b) the $PbCl_2 + HCl + H_2O$ system from 0 to 100 °C. Experimental data are from Linke and Seidell (1965), Clever and Johnston (1980), Tan et al. (1987), and Mgaidi et al. (1991).

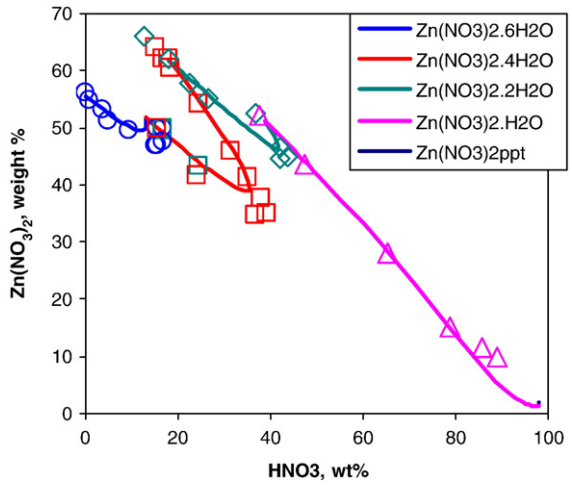

Fig. 8. Solubility of $Zn(NO_3)_2$ in $HNO_3 + H_2O$ mixtures at 25 °C. Experimental data are from Linke and Seidell (1965).

on P_{CO_2} may also depend on other system variables such as pH, temperature, and the salt concentration. This is demonstrated in Fig. 10 in which the solubility of $PbCO_3$ appears to decrease with CO_2 partial pressure in the presence of additional components. The trend shown in Fig 10a is due to the combined effects of pH and CO_2 partial pressure. At fixed pH, a rise in CO_2 partial pressure tends to depress the solubility of carbonates primarily because of the increased formation of carbonate ions and the subsequent common-ion effect. This is in contrast with Fig. 9, in which the rise in CO_2 partial pressure causes a simultaneous acidification of the solution. In Fig. 10b, the change of the $PbCO_3$ solubility with the concentration of $KHCO_3$ is a combination of the common-ion effect (which results in a decreased solubility at low salt concentrations) and ion pair formation between Pb^{+2} and CO_3^{-2} or HCO_3^- (resulting in an increased solubility at higher salt concentrations). The decrease in solubility with increasing P_{CO_2} is due to the shift of the dissolution reaction (cf. Eq. (7)) to the left upon the addition of CO_2 (cf. Eq. (8)):

$$PbCO_3(s) + KHCO_3 = Pb(CO_3)_2^{-2} + H^+ + K^+ \quad (7)$$

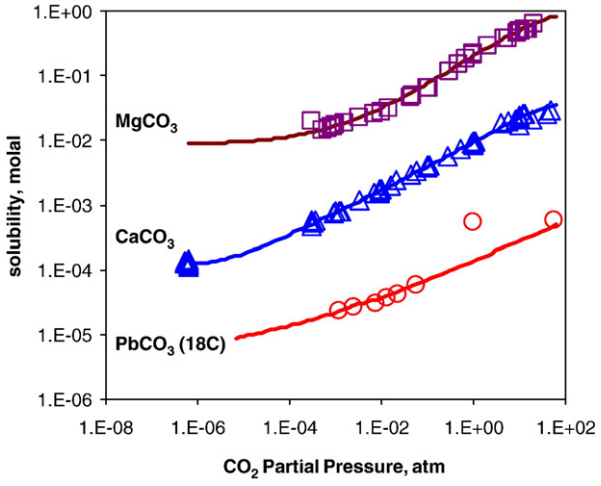

Fig. 9. Calculated and experimental solubilities in three MCO_3–CO_2–H_2O systems (M = Pb, Ca, Mg) at 25 °C. Experimental data are from Linke and Seidell (1965), Wolf et al. (1989), Plummer and Busenberg (1982), MacDonald and North (1974), Moshkina et al. (1977), Ponizovskii et al. (1979), and Rykova and Shternina (1967).

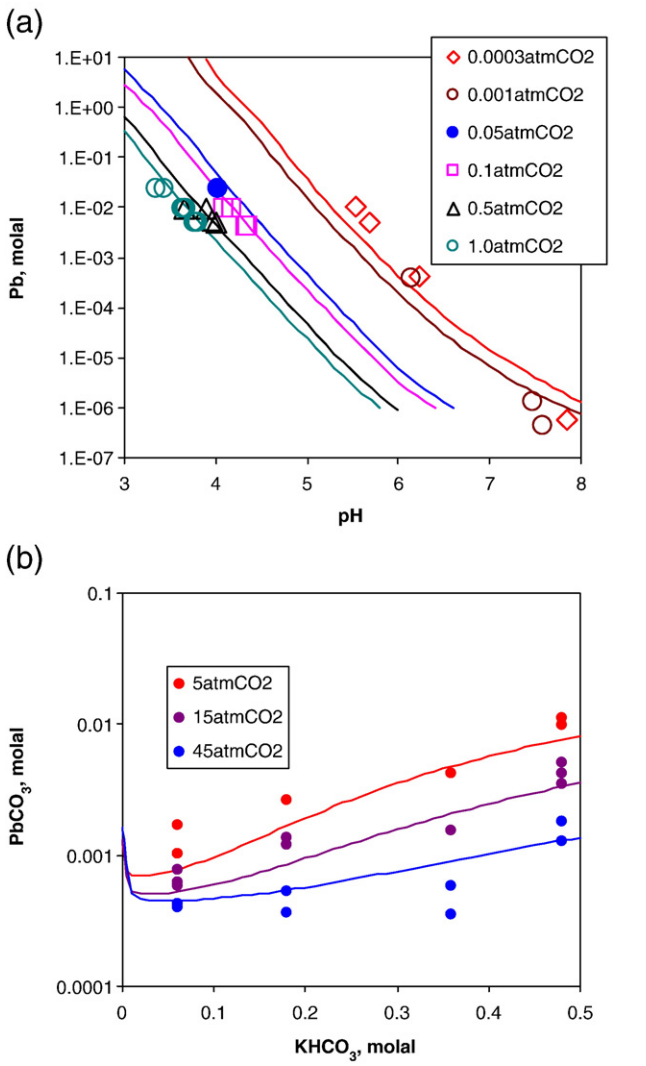

Fig. 10. Calculated and experimental solubilities for $PbCO_3$ (cerussite) at various partial pressures of CO_2 in (a) aqueous 0.3 m $NaClO_4$ solutions at 25 °C and (b) aqueous $KHCO_3$ solutions containing 0.1 m NaCl at 300 °C. Experimental data are from Bilinski and Schindler (1982) and Baranova and Barsukov (1965).

$$CO_2 + H_2O = HCO_3^- + H^+. \quad (8)$$

The correct representation of solubility data demonstrates that the model accurately predicts the nonideality for all of the investigated systems.

It should be noted that the model parameters developed in this study have been verified for all related systems. For example, all parameters that are pertinent to the $PbCl_2 + HCl + H_2O$ system, including binary interaction parameters and standard-state thermochemical data for aqueous complexes and solids, are also applicable to the $PbCl_2 + NaCl + H_2O$ system, and vice versa. These parameters are reported in Table 1. At low salt or acid concentrations, the solubilities of the solid phases in these systems are low (e.g. less than 0.1 m at $T < 100$ °C), and are primarily accounted for by the standard-state thermochemical properties ($\Delta_f G^0$, S^0, C_p^0), supplemented by the long-range electrostatic contribution to activity coefficients from the Pitzer–Debye–Hückel formula. As the acid or salt concentration increases, the solubility rises due to the formation of complexes, and interactions between H_3O^+ or Na^+ and the complex species (e.g. $PbCl_3^-$ or $PbCl_4^{-2}$) are introduced to represent the increasing solubilities. The interactions are introduced only for species that appear in significant amounts in the equilibrium solutions.

Table 1
Model parameters for the $PbCl_2 + HCl + H_2O$ and $PbCl_2 + NaCl + H_2O$ systems.

Binary parameters in Eqs. (4) and (5)[a,b]	Parameters for aqueous species[c]
$b_0(H_3O^+, PbCl_3^-) = b_0(H_3O^+, PbCl_4^{-2}) = 103.323$	Pb^{+2}: $\Delta_f G^0 = -23.890$, $S^0 = 17.5728$[d]
$b_2(H_3O^+, PbCl_3^-) = b_2(H_3O^+, PbCl_4^{-2}) = -25{,}084.0$	$PbCl^+$: $\Delta_f G^0 = -163.385$, $S^0 = 117.152$[d]
$c_0(H_3O^+, PbCl_3^-) = c_0(H_3O^+, PbCl_4^{-2}) = -159.461$	$PbCl_2^0$: $\Delta_f G^0 = -297.901$, $S^0 = 196.648$[d]
$c_2(H_3O^+, PbCl_3^-) = c_2(H_3O^+, PbCl_4^{-2}) = 32{,}575.4$	$PbCl_3^-$: $\Delta_f G^0 = -427.396$, $S^0 = 246.856$[d]
$b_0(Na^+, PbCl_4^{-2}) = -31.3926$	$PbCl_4^{-2}$: $\Delta_f G^0 = -558.041$, $S^0 = 276.144$[b]
$b_2(Na^+, PbCl_4^{-2}) = 30{,}104.3$	Parameters for solid species[c]
$c_2(Na^+, PbCl_4^{-2}) = -26{,}488.2$	$PbCl_2$: $\Delta_f G^0 = -313.358$, $S^0 = 133.57$[b]

[a] Parameters not listed are set to be zero.
[b] Values are determined from this study.
[c] Units are in $kJ.mol^{-1}$ for $\Delta_f G^0$, $J.mol^{-1}.K^{-1}$ for S^0.
[d] Values are taken from Sverjensky et al. (1997) and Shock and Helgeson (1988).

5. Conclusions

A recently developed comprehensive mixed-solvent electrolyte model has been applied to calculate phase equilibria in multicomponent systems containing salts and acids in wide concentration and temperature ranges. The model has been shown to be very useful for reproducing complex solid–liquid equilibrium diagrams for selected transition and post-transition metal systems containing salts and acids over wide concentration ranges including water-depleted environments as well as classical aqueous systems. Compared to other existing thermodynamic models, this model has an extended applicability range with respect to salt concentration (i.e., from infinite dilution to the fused salt limit), types of solvent components (either aqueous or non-aqueous or mixed solvents), and environmental conditions (temperatures up to 300 °C and corresponding pressures), in addition to its capability of predicting equilibrium speciation. Thus, the model can be used to predict the ranges of physicochemical conditions for mineral deposition, and the predicted speciation results can be of value for understanding the mechanisms of transport of metals and deposition of minerals in natural environments for mineral exploration.

Acknowledgements

This work was supported by Alcoa, Chevron, DuPont, Mitsubishi Chemical, Rohm & Haas and Shell.

References

Abrams, D.S., Prausnitz, J.M., 1975. Statistical thermodynamics of liquid mixtures: a new expression for the excess Gibbs energy of partly or completely miscible systems. AIChE Journal 21, 116–128.
Almkvist, G., 1918. Bestimmung der Löslichkeit einiger Metallhydroxyde in Wasser. Zeitschrift für anorganische und allgemeine Chemie 103, 240–242.
Anderko, A., Wang, P., Rafal, M., 2002. Electrolyte solutions: from thermodynamic and transport property models to the simulation of industrial processes. Fluid Phase Equilibria 194–197, 123–142.
Anderson, G.M., 1962. The solubility of PbS in H_2S–water solutions. Economic Geology 57, 809–828.
Azimi, G., Papanggelakis, V.G., Dutrizac, J.E., 2007. Modelling of calcium sulphate solubility in concentrated multi-component sulphate solutions. Fluid Phase Equilibria 260, 300–315.
Azimi, G., Papanggelakis, V.G., Dutrizac, J.E., 2008. Development of an MSE-based chemical model for the solubility of calcium sulphate in mixed chloride–sulphate solutions. Fluid Phase Equilibria 266, 172–186.
Baes, C.F., Mesmer, R.E., 1976. The Hydrolysis of Cations. John Wiley & Sons, New York.
Baranova, N.N., Barsukov, V.L., 1965. Transport of lead by hydrothermal solutions in form of carbonate complexes. Geochemistry International 2, 802–809.
Barrett, T.J., Anderson, G.M., 1982. The solubility of sphalerite and galena in NaCl brines. Economic Geology 77, 1923–1933.
Barrett, T.J., Anderson, G.M., 1988. The solubility of sphalerite and galena in 1–5 m NaCl solutions to 300 °C. Geochimica et Cosmochimica Acta 52, 813–820.
Bilinski, H., Schindler, P., 1982. Solubility and equilibrium constants of lead in carbonate solutions (25 °C, I = 0.3 mol/dm^3). Geochimica et Cosmochimica Acta 46, 921–928.
Clever, H.L., Johnston, F.J., 1980. The solubility of some sparingly soluble lead salts: an evaluation of the solubility in water and aqueous electrolyte solution. Journal of Physical and Chemical Reference Data 9, 751–784.
Gayer, K.H., Garrett, A.B., 1949. The equilibria of nickel hydroxide, $Ni(OH)_2$, in solutions of hydrochloric acid and sodium hydroxide at 25. Journal of the American Chemical Society 71, 2973–2975.
Gayer, K.H., Woontner, L., 1952. Hydrolysis of cobalt chloride and nickel chloride at 25. Journal of the American Chemical Society 74, 1436–1437.
Gruszkiewicz, M.S., Palmer, D.A., Springer, R.D., Wang, P., Anderko, A., 2007. Phase behavior of aqueous Na–K–Mg–Ca–Cl–NO_3 mixtures: isopiestic measurements and thermodynamic modeling. Journal of Solution Chemistry 36, 723–765.
Helgeson, H. C., Kirkham, D.H., 1974. Theoretical prediction of the thermodynamic behavior of aqueous electrolytes at high pressures and temperatures. I & II. American Journal of Science 274, 1089–1198 & 1199–1261.
Helgeson, H.C., Kirkham, D.H., 1976. Theoretical prediction of thermodynamic properties of aqueous electrolytes at high-pressures and temperatures; III. Equation of state for aqueous species at infinite dilution. American Journal of Science 276, 97–240.
Helgeson, H.C., Kirkham, D.H., Flowers, G.C., 1981. Theoretical prediction of the thermodynamic behavior of aqueous electrolytes by high pressures and temperatures; IV, calculation of activity coefficients, osmotic coefficients, and apparent molal and standard and relative partial molal properties to 600 degrees C and 5 kb. American Journal of Science 281, 1249–1516.
Kosinski, J.J., Wang, P., Springer, R.D., Anderko, A., 2007. Modeling acid–base equilibria and phase behavior in mixed solvent electrolyte systems. Fluid Phase Equilibria 256, 34–41.
Linke, W.F., Seidell, A.S., 1965. Solubilities of Inorganic and Metal Organic Compounds K–Z, Volumes I and II, 4th Edition. American Chemical Society, Washington.
Liu, H., Papangelakis, V.G., 2005. Thermodynamic equilibrium of the O_2–$ZnSO_4$–H_2SO_4–H_2O system from 25 to 250 °C. Fluid Phase Equilibria 234, 122–130.
Liu, H., Papangelakis, V.G., 2006. Solubility of Pb(II) and Ni(II) in mixed sulfate–chloride solutions with the mixed solvent electrolyte model. Industrial & Engineering Chemistry Research 45, 39–47.
MacDonald, R.W., North, N.A., 1974. The effect of pressure in the solubility of $CaCO_3$, CaF_2, and $SrSO_4$ in water. Canadian Journal of Chemistry 52, 3181–3186.
Mattigod, S.V., Rai, D., Felmy, A.R., Rao, L., 1997. Solubility and solubility product of crystalline $Ni(OH)_2$. Journal of Solution Chemistry 26, 391–403.
McDowell, L.A., Johnston, H.L., 1936. The solubility of cupric oxide in alkali and second dissociation constant of cupric acid. The analysis of very small amount of copper. Journal of the American Chemical Society 58, 2009–2014.
Mgaidi, A., Furst, W., Renon, H., 1991. Representation of the solubility of lead chloride in various chloride solutions with Pitzer model. Metallurgical and Materials Transactions B 22, 491–498.
Moshkina, I.A., Poroshina, I.A., Samsonova, T.I., Worsina, I.A., 1977. The stable and metastable equilibriums in the system $CaCl_2$–$CaCO_3$–H_2O at 25 °C and PCO_2 about 1 atm. Izvestiya Sibirskogo Otdeleniya Akademii Nauk SSSR Seriya Khimicheskikh Nauk 5, 122–126.
Muller, E., 1923. Das System Kupferoxyd. Kupferhydroxyd, Cuprit, Natronlauge, Zeitschrift fur Physikalische Chemie 105, 73–118.
Paige, C.R., Kornicker, W.A., Hileman Jr., O.E., Snodgrass, W.J., 1992. Modelling solution equilibria for uranium ore processing: the $PbSO_4$–H_2SO_4–H_2O and $PbSO_4$–Na_2SO_4–H_2O systems. Geochimica et Cosmochimica Acta 56, 1165–1173.
Petrov, A., Palmer, D., 2000. Evaluation of models for solubility and volatility of copper compounds under steam generation conditions. Proceedings of the 13th International Conference on the Properties of Water and Steam, pp. 821–827.
Pitzer, K.S., 1991. Activity Coefficients in Electrolyte Solutions, 2nd ed. CRC Press, Boca Raton, FL.
Plummer, L.N., Busenberg, E., 1982. The solubilities of calcite, aragonite and vaterite in CO_2–H_2O solutions between 0 and 90C, and an evaluation of the aqueous model for the system $CaCO_3$–CO_2–H_2O. Geochimica et Cosmochimica Acta 46, 1011–1040.
Ponizovskii, A.A., Orlova, V.T., Lepeshkov, I.N., 1979. Solubility of calcite in aqueous solutions of salts at 25 C and a CO_2 pressure of about 0.02 atm. Russian Journal of Inorganic Chemistry 24, 1875–1877.
Qiu, L., Klimas, S., Snaglewski, A.P., Grondin, J.M., 2006. Solubility and mobility of Pb-bearing species under Candu steam generator conditions. 5th CNS International Steam Generator Conference Toronto.
Rafalskiy, R.P., Masalovich, A.P., 1981. Determination of the instability constants of lead chloride complexes at elevated temperatures. Geochemistry International 18, 158–174.
Rykova, G.A., Shternina, E.B., 1967. System $CaCO_3$–K_2SO_4–H_2O–CO_2 at 25 °C and PCO_2 about 1 atm. Zhurnal Neorganicheskoi Khimii 12, 2789–2795.
Shock, E.L., Helgeson, H.C., 1988. Calculation of the thermodynamic and transport properties of aqueous species at high pressures and temperatures: correlation algorithms for ionic species and equation of state predictions to 5 kb and 1000 °C. Geochimica et Cosmochimica Acta 52, 2009–2036.
Sverjensky, D.A., Shock, E.L., Helgeson, H.C., 1997. Prediction of the thermodynamic properties of aqueous metal complexes to 1000 °C and 5 kb. Geochimica et Cosmochimica Acta 61, 1359–1412.
Tan, K.G., Bartels, K., Bedard, P.L., 1987. Lead chloride solubility and density data in binary aqueous solutions. Hydrometallurgy 17, 335–356.
Tremaine, P.R., Leblanc, J.C., 1980. The solubility of nickel oxide and hydrolysis of Ni^{2+} in water to 573 K. The Journal of Chemical Thermodynamics 12, 521–538.
Wang, P., Anderko, A., Young, R.D., 2002. A speciation-based model for mixed-solvent electrolyte systems. Fluid Phase Equilibria 203, 141–176.
Wang, P., Springer, R.D., Anderko, A., Young, R.D., 2004. Modeling phase equilibria and speciation in mixed-solvent electrolyte systems. Fluid Phase Equilibria 222–223, 11–17.

Wang, P., Anderko, A., Young, R.D., Springer, R.D., 2005. A comprehensive model for calculating phase equilibria and thermophysical properties of electrolyte systems in "Computational Analysis in Hydrometallurgy". In: Dixon, D.G., Dry, M.J. (Eds.), Proceedings of the International Symposium on Computational Analysis in Hydrometallurgy, 35th Annual Hydrometallurgy Meeting. Canadian Institute of Mining, Metallurgy and Petroleum, Montreal, Canada, pp. 259–273.

Wang, P., Anderko, A., Springer, R.D., Young, R.D., 2006. Modeling phase equilibria and speciation in mixed-solvent electrolyte systems: II. Liquid–liquid equilibria and properties of associating electrolyte solutions. Journal of Molecular Liquids 125, 37–44.

Wolf, M., Breitkopf, O., Puk, R., 1989. Solubility of calcite in different electrolytes at temperatures between 10 and 60C and at CO_2 partial pressures of about 1kPa. Chemical Geology 76, 291–301.

Var'yash, L.N., 1986. Hydrolysis of Cu(II) at 25–350C. Geochemistry International 23, 82–92.

Ziemniak, S.E., Jones, M.E., Combs, K.E.S., 1989. Solubility and phase behavior of nickel oxide in aqueous sodium phosphate solutions at elevated temperatures. Journal of Solution Chemistry 18, 1133–1152.

Ziemniak, S.E., Goyette, M.A., 2004. Nickel(II) oxide solubility and phase stability in high temperature aqueous solutions. Journal of Solution Chemistry 33, 1135–1159.